Synthesis and Characterization of Kaolin Assisted Metal Nanocomposite and its Tremendous Adsorptive and Photo Catalytic Applications
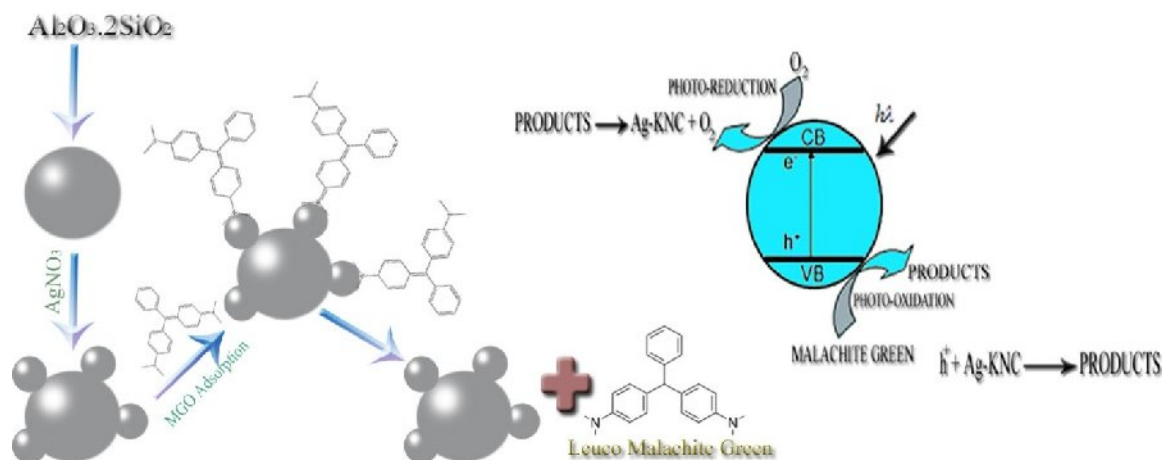
Hajira Tahir*, Muhammad Saad, Atika Saud and Uzma Saleem
Department of Chemistry, University of Karachi, Karachi, Pakistan.
hajirat@uok.edu.pk*

Summary: The present work demonstrates the synthesis of Kaolin assisted Ag nanocomposite (Ag-KNC) by co-precipitation method. The surface morphology of them was studied through SEM and chemical constituents by EDS techniques. The removal of efficaciousness of Ag-KNC was tested by Malachite Green Oxalate (MGO) dye through batch adsorption and photocatalytic strategies. The sorption experiments were preceded under the optimized conditions like amount of adsorbent, stay time and pH. The feasibility of the process was determined by employing Freundlich, Langmuir and D-R (Dubinin –Radushkevich) adsorption isotherms. The pH at point of zero charge (pH_{pzc}) was conjointly calculable to work out the surface neutrality of the system.

The salt effect for the removal of MGO dye was investigated. Thermodynamic parameters like free energy (ΔG^o), entropy (ΔS^o) and enthalpy (ΔH^o), of the system was investigated. Adsorption Kinetic was resolute by Intra particle diffusion (IPD) and Boyd's models.

An attempt was made to prepare (Ag-KCN) nanophoto catalyst by UV light assisted degradation of Malachite Green Oxalate (MGO) dye. They were prepared by the reduction of Ag^+ ion under alkaline conditions on kaolin surface. The photo degradation (PD) process was initiated by photo generated electrons. The present study recommended that projected strategies were successfully applied for the remediation of environmental problems.

Mechanism for the synthesis of Ag-KNC and its Adsorption and Photocatalytic degradation of MGO Dye

Introduction

The nano fabrications processes receive attention due to their intrinsic size-dependent properties compeered to other conventional methods [1, 2]. It has been reported that changes in critical size enhances the materials characteristic [3]. In this context, the surface area/volume quantitative relation of materials employed within the preparation of nanocomposite was determines to grasp the structural properties of them [4].

Nanocomposite comprises of nanoparticles and nanofillers. They distributed into matrix of standard materials [5]. They can be classified into metal oxide, polymer based, carbon nanotubes and novel metal bases. Carbon nanotube based nanocomposites have low masses and display excellent mechanical and thermal properties [6 - 9]. Apart from their applications they show glorious removal efficiencies for numerous metals and dyes from waste product [10].

---

*To whom all correspondence should be addressed.

The metal nanoparticles (NPs) have outstanding physical and chemical properties proved from worldwide investigations [11]. The Silver nanoparticles (Ag-NPs) are widely used as antibacterial agents, catalysts, photo catalysts, photosensitive components and the surface enhancer [12, 13].

It has been reported that some metal oxides act as efficient photocatalysts and are able to be used for the degradation of toxic organic compounds in air or water under UV light irradiation. Nanophotocatalyst notice applications in environmental remediation, sterilization, hydrogen production and renewable energy. They has been used with success for the remediation of hazardous materials such as industrial effluents, colorants and dyes. They are non-toxic, chemically and thermally stable, inexpensive and stable to corrosion within the presence of water and chemicals [14, 15].

Whilst they were exposed to light afterward the valance band electron absorb energy and transfer it to conduction band and produces an electron-hole pair [16]. They are generated by the ultraviolet-visible light irradiation (h^+_{vb}) after that they interact with H_2O to provide $OH^{\cdot}$ and e_{eb}. They conjointly react with dissolved O_2 to give $^{\cdot}O_2$ and these active radicals decompose the dye [17-20].

Dyes are considerably utilized in varied industries. Customarily they are toxic and some of them are mutagenic and carcinogenic [21]. The effluent from diverse industrial units causes contamination of water bodies [22]. They not solely contaminate the water resources however their persistence disturbs the photosynthetic activity which is an essential feature of contaminated water bodies [23]. The adsorbents like activated carbon [24] chitosan, [25] fly ash [26] are utilized by scientists and showing their removal efficiencies for the diminution of waste water.

Kaolin is the foremost common clay minerals found on the surface of the earth. The general structure of the kaolinite group is composed of silicate sheets (Si_2O_5) banded to aluminum oxide/hydroxide layers ($Al_2(OH)_4$). Ag is an important inorganic material that has wide applications perspective in chemical process [27-29].

The significance of this study is the novel initiative to combine the silver nanoparticle with inexpensive kaolin clay and utilization of them as adsorbent and photo catalyst for the degradation of effluent (MGO) dye within the presence of visible light irradiation. The objective of this study is to look at the adsorption and photocatalytic degradation of MGO dye removal within the presence of kaolin assisted Ag nanophoto catalyst.

The current study represents unified approach for the synthesis of nanocomposites with increased properties by incorporating kaolin clay. The results discovered that they have tremendous potential for the removal of dyes and these ways are useful for the redress of waste water at wide scale [30].

Experimental

Methods

Synthesis of Nanocomposits

The synthesis of (Ag-KNC) was carried out by means of baked form of $Al_2O_3.2SiO_2$ (Kaolin). Afterwards 2.0 g of it was mixed with 200 ml C_2H_5OH (w/v) with constant stirring at 120 rpm for 2 hours in a shaking incubator. Succeeding that Kaolin was well dispersed and NaOH (5% w/v) added within the reaction mixture under constant stirred conditions. After that it was left for 24 hours at room temperature. Later than, 30 ml of $AgNO_3$ (7.6 g L^{-1} in C_2H_5OH) was added at the rate of 0.5 ml/min. Afterward the residues were washed over a Buchner funnel fitted to a vacuum assembly. The precipitate was filtered by several washings with deionized water to get neutral pH and then they were dried in ambient conditions. The synthesized composite were labeled as (Ag-KNC) and they were used for further studies [31].

Characterization of Ag-KNC

The nanocomposites of (Ag-KNC) were characterized by SEM and EDS (Jeol JSM-6380A analytical scanning microscope) techniques.

Removal of MGO Dye

The batch adsorption experiments were preceded under the effect of certain adsorption parameters like dosage of Ag-KNC, pH, stay time, pH at point of zero charge (pH_{ZPC}) and salt effect. These experiments were preceded by utilizing 500 mg/L solution of MGO dye and temperatures were varied from ($25\text{-}40 \pm 1°C$). The working standards were prepared to optimize the λ_{max} as represented in Fig. 1.
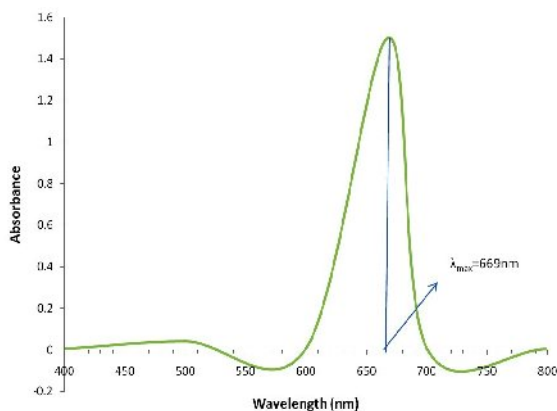
Fig. 1:   The working standards were prepared by standard addition method.

Ag-KNC dosage

The Ag-KNC dosage was varied from (0.1 to 2.0g)/ 50 mL of MGO dye. The content was shaken at 200 rpm at 298K temperature. After the specified time period it was filtered and determines its concentration.

Stay Time Variation

The stay time was varied from 5 to 60 min.,around 50mL of MGO solution was agitated with 0.5g of Ag-KNC. The content was shaken for the variable time intervals (5.0 to 60 min.) at 200 rpm and 298K temperature.

pH of the system

The pH of the system was adjusted from (2-12). About0.5g,of Ag-KCN was added in 50mL of dye solution at specified pH and it was shaken at 200rpm on 298K temperature. The concentration of filtrate after precise time period was recorded.

Adsorption Isotherms

The Freundlich, Langmuir and Dubinin Radushkevich (D-R) adsorption isotherms were elicited for Kaolin and (Ag-KNC) systems under the effect of optimized parameters within the temperatures ranges 298 to 313K.

pH at Point of Zero Charge(pH_{ZPC})

The pH at which total number of charges on the surface of Ag-KNC becomes zero is called pH of point zero charge (pH_{ZPC}) [36] .The pH drift method was adopted to investigate the effect of pH at pH_{ZPC}

of Ag-KNC. The pH was adjusted between 2 to 12. About 50 mL of respective pH solutions with optimum amount of Ag-KNC was kept at room temperature for 48 hours. The stabilize pH was recorded after 24 and 48 hours [32].

Effect of Salts Concentration

Effect of salts KCl concentration on adsorption was studied and its interactions with adsorbents and adsorbate was monitored.

Photocatalytic Activity

The degradation of MGO dye was preceded under UV light irradiation in the presence of Ag-KNC. The light source of 15W medium pressure, sodium lamp was used. About 0.5g of Ag-KNC was added in 100mL of 150mg.L^{-1} MGO dye and the content was stirred for 30min in dark place. After word it was placed under the influence of UV irradiation for two hour. At the interval of 15min 5ml of aliquots was drawn. Subsequent to centrifugation the left over concentration was analyzed by UV-spectrophotometer.

Kinetics of Adsorption

The rate of adsorption process was determined by Lagergren's pseudo first order and Ho-McKay's pseudo-second order models.

Result and Discussion

Scanning Electron Microscopic Analysis

It was pragmatic by SEM images that the sizes were varied between 50-100 nm which appears brighter and supported by darker surface of $Al_2O_3.2SiO_2$ as shown in Fig. 2.

The empty sites present on the surface of Ag-KNC provide active sites for the adsorption of MGO dye molecules.
EDS Analysis

Energy Dispersive X-Ray spectroscopy is a popular tool to extract the chemical information about the analyte. The EDS spectrum of Ag-KNC is shown in Fig. 3**.** It is evident from the Fig that the nanocomposite is composed primarily of Oxygen, Aluminium, Silicon, and Silver[33].
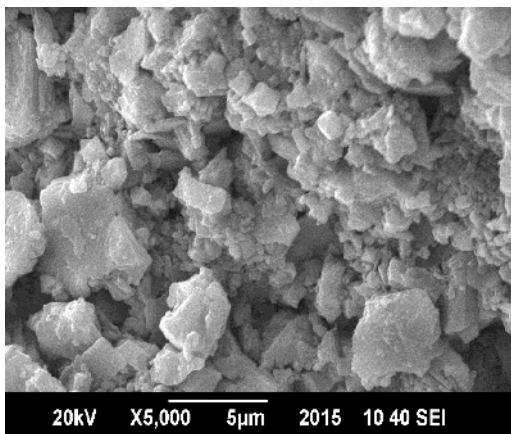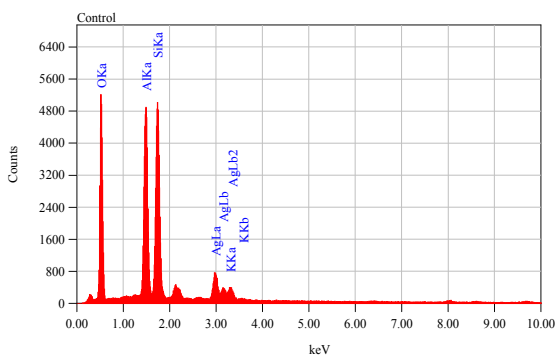
Fig. 2:   SEM image of Ag-KNC.

Fig. 3:   EDS spectrum of Ag-KNC.

Batch Adsorption Experiments

The removal of (MGO) dye was preceded by Ag-KNC and Kaolin under the effect of optimum amount of adsorbent, pH, dye concentration, shaking time, electrolytic concentration and temperature. The effect of P^H at point of zero charge, thermodynamic and kinetic studies was also conducted by using Kaolin and Ag-KNC.

Effect of Ag-KNCdosage

It was observed that the adsorption efficiency was increased as the Ag-KNC dosageraises from 0.1 to 2.0 g. The removal efficiency was enhanced until it reaches a saturation point, after that the increase in adsorbent dosage does not change the percentage removal. The increase in adsorption rate with the adsorbent dosage attributes the availability of more adsorption sites [34]. The greatest removal efficiency was observed in case of MGO-Ag-KNC compared to MGO-kaolin system.
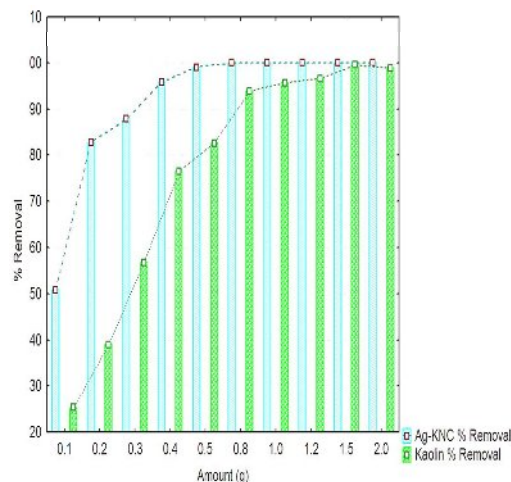

Fig. 4:   Optimization of Amount of MGO-kaolin, and MGO-Ag-KNC systems.

Effect of PH

The effect of pH on the adsorption of dye was investigated shown in Fig. 5. The pH was varied from 2 to 10[30]. Moreover the removal of MGO was increased with the augment in pH and maximum value was observed at pH 5.0, it show that it effect on the binding sites of the Ag-KCN. The observed trend also be explain by the surface charge of adsorbent. Depending on the solution pH, the adsorbent surface undergoes protonation and also deprotonation. The highly positive charge density makes the MGO adsorption more favorable due to electrostatic attraction. However, the deprotonated species under goelectrostatic repulsion of negative charged dye molecules which causes decreased in dye adsorption [35].
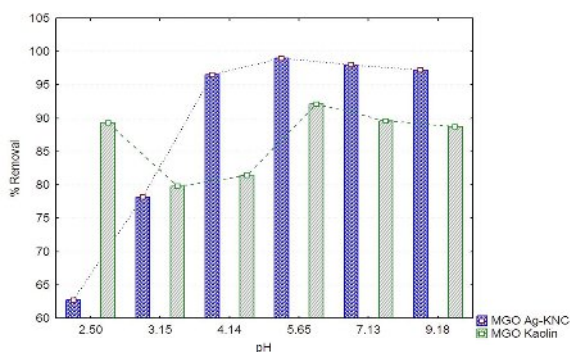

Fig. 5:   Optimization of pH of MGO-kaolin, and MGO-Ag-KNC systems.

Effect of Stay Time

The process of adsorption of MGO was enhanced by increase in stay time. It was observed that removal efficiencies were reaches to the optimum value when the equilibrium between adsorbate and adsorbent was established [36, 37]. The adsorption capacity of MGO was observed for kaolin system about 88.42 % at 30 min, while for Ag-KNC it was found to be 95% within 10 min as shown in Fig. 6.
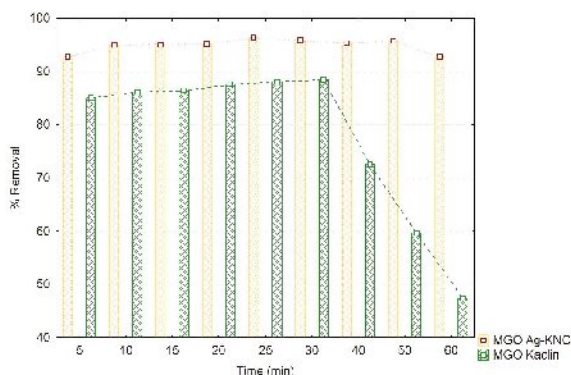

Fig. 6:   Optimization of Stay Time of MGO-kaolin and MGO-Ag-KNC systems.

Effect of pH_{ZPC}

It was observed that at variable pHs of the system it was level off at limiting value about 6.2 and 3.6 after 24 and 48 hours for Kaolin and Ag-KNC systems. It appears that some sort of acid base equilibrium was established between the adsorbent and the aqueous phase which depends on the number of replaceable protons present at the surface of adsorbent [38]. The pH_{ZPC} value of Kaolin and Ag-KNC are shown in Fig. 7 (a, b). It was observed that neutralization point observed at pH of 4.0.

Adsorption Isotherms

The adsorption isotherm models were commissioned on the experimental data.

Adsorption isotherms are significant for the industrial applications particularly for determining the best fitted isotherm model. The adsorption behavior between the adsorbate and adsorbent is described by Langmuir, Freundlich and D-R isotherm models. The calculated values of constants are provided in Table-1. The experimental data represented that Langmuir Model at 308K is a best fitted isotherm for MGO-Kaolin and MGO-Ag-KCN systems as affirmed by the high R^2 values. At this particular temperature, the values of V_m for MGO-Kaolin and MGO-Ag-KCN were determined to be

8.375 mg. g^{-1} and 10.75 mg. g^{-1} respectively. Moreover the values of Langmuir constant K for MGO-Kaolin and MGO-Ag-KCN were 2.659 L. mg^{-1} and 0.5864 L. mg^{-1} respectively [39].
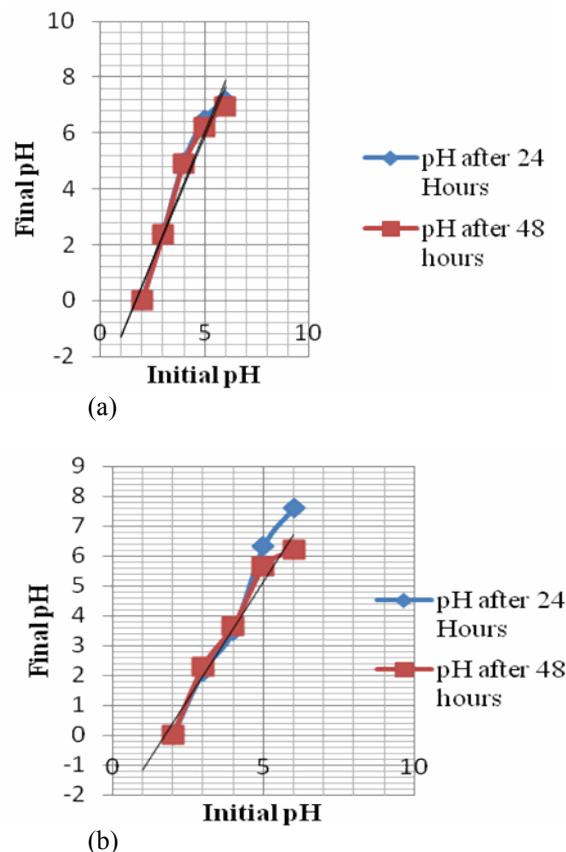

(a)

(b)

Fig. 7:   pH_{ZPC} of (a) kaolin and (b) Ag-KNC.

The multilayer adsorption is studied by Freundlich isotherm. The value of adsorption constant n was evaluated to be 1-10 as given in the Table-1. It represents the favorable nature of the processes except for MGO-Ag-KNC at 313K.It was determined to be 42.55 it is clear from the result that the R^2 value lie as 0.0045. It indicated that this isotherm model is not followed at such high temperature.

The magnitude of E by Dubinin Radushkevich isotherm reveals the nature of the adsorption process. If the value of ε is lesser than 8.0 kJ mol^{-1}, it represents the physisorption process. They lies between 8-16 kJ mol^{-1} then it represents ion exchange phenomenon and if it lies between 20-40 kJ mol^{-1} then it represents chemical adsorption.The ε values were determined to be less than8.0kJ mol^{-1}. It represents that the adsorption of MGO on Kaolin and Ag-KCN is physical phenomena [40-42].

Table-1: Isotherm studies and their corresponding coefficient values.

Isotherm Models		Parameters	Temperature (K)							
			298		303		308		313	
			Kaolin (K)	Ag-KCN	Kaolin	Ag-KCN	Kaolin	Ag-KCN	Kaolin	Ag-KCN
Freundlich $Log\frac{x}{m} = Log K + \frac{1}{n} Log Ce$	It is empirical equation used to describe heterogeneous system. Where X/m is the amount adsorbed per unit mass of the adsorbent, Ce is the equilibrium concentration and n and K are Freundlich constants [40]. The amount of MGO adsorbed (X/m) was calculated as : $$\frac{X}{m} = \frac{(C_o - C_e)V}{m}$$ Where C_o and C_e are the initial and equilibrium concentrations of MGO (mg. L^{-1}), m is the mass of Ag-KNC (g), and V is the volume of dye solution (L).	n	4.968	6.211	7.321	3.110	5.608	5.033	5.519	42.55
		K_F(L mg^{-1})	6.065	9.922	9.995	6.420	9.143	9.294	8.525	10.96
		R^2	0.3105	0.2559	0.2471	0.6726	0.3718	0.4000	0.7233	0.0045
Langmuir $\left(\frac{C_e}{\frac{X}{m}}\right) = \left(\frac{1}{KV_m}\right) + \left(\frac{C_e}{V_m}\right)$	Langmuir isotherm model defines finite number of active sites which are homogeneously distributed over the surface of the adsorbent. This model represented that, there was no interaction between adsorbed molecules and have the same affinity for the mono layer adsorption process [41]. Where Vm is the volume of monolayer adsorption capacity and K is the Langmuir constant related to Free energy.	V_m(mg g^{-1})	10.54	6.042	14.18	7.102	8.375	10.75	7.981	4.398
		K (L mg^{-1})	0.3961	0.1913	0.1504	0.4937	2.659	0.5864	0.2992	0.2063
		R^2	0.9963	0.9902	0.9984	0.9986	0.9995	0.9988	0.9962	0.9944
Dubinin Radushkevich $Ln\frac{x}{m} = \ln X_m - K\varepsilon^2$	D-R isotherm is applied to study the nature of adsorption whether it is physical or chemical. The linear form is represented in the left column where X_m is the monolayer capacity of adsorbent, K is a constant related to adsorption energy; ε is adsorption potential, which can be calculated as [42] $$\varepsilon = RT\ Ln\left(1 + \frac{1}{C_e}\right)$$ E provides information about the physical or chemical nature of adsorption process and it can be calculated as: $E=(2K)^{-0.5}$	ε(kJ mol^{-1})	0.2673	1.581	1.000	0.5000	1.118	1.581	2.673	1.118
		X_m	16.89	16.31	20.18	25.23	19.00	16.55	16.46	12.53
		K (10^{-7})	70	2	5	20	4	2	0.7	4
		R^2	0.8506	0.1031	0.8329	0.9617	0.6652	0.1915	0.8048	0.0242

Salt Effect on the Adsorption of Dye

The salt molecules are able to dissociate in to its ions resulting increase in solvation. The presence of KCl electrolyte produces opposing effects in term of adsorption efficiency. The electrostatic interaction between dye molecules and adsorbent was decreased, representing increase in the degree of dissociation of MGO by facilitating the protonation process [43, 44]. The results are shown in Fig. 8. It shows that the adsorption efficiency was influenced by the concentration of electrolytic species. There are two dominating effects acting in opposite directions. At lower salt concentrations, electrostatic effects dominate, leading to an increased capacity, while at higher salt concentrations, water cluster formation has the strongest influence.
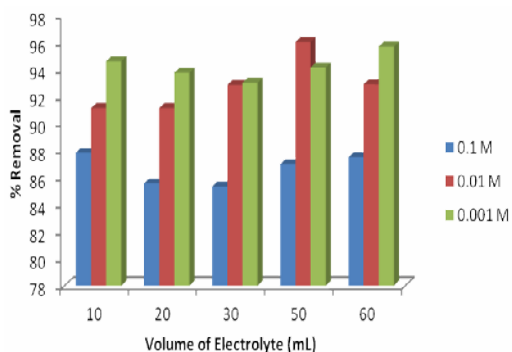

Fig. 8:　　Effect of Salt concentration for the MGO dye.

Intra – Particle Diffusion Model

IPD model was proposed by Weber and Morris and applied for the analysis of adsorption kinetics [45]. There is a functional relationship of the adsorption process while the adsorption uptake was almost proportional with $t^{1/2}$ rather than with the contact time (t), it was experimentally determined by IPD model. The Weber and Morris Intra particle diffusion model is represented as:

$$log\ q_t\ =\ log\ K_{id}\ +\ 0.5\ log\ t$$

where k_{id} is the intra-particle diffusion rate constant, which was obtained from the slope of the linearized plot of $log\ q_t$ vs. t as shown in Fig. 9. The value obtain from intercept describe the thickness of the boundary layer which represented that the boundary layer effect increases. Moreover the positive values of slope representing the controlled adsorption process.
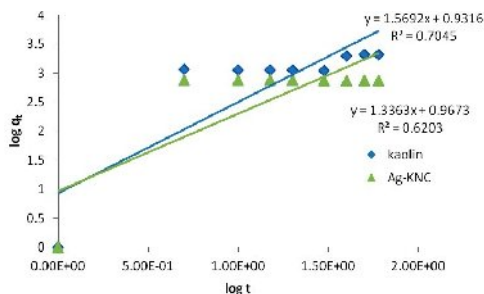

Fig. 9:　　Intra particle diffusion model of kinetics for Kaolin and Ag-KNC Systems.

The Boyd Kinetics Model

The Boyd's model suggested the slow step adsorption process. It is represented as [46]:

$$F = 1 - \frac{6}{\pi^2}\ exp(-B_t)$$

$$B_t = -0.4977 - ln(1 - F)$$

where F represents the fraction of solute adsorbed on adsorbent at time, t (min), which was calculated as:

$$F = \frac{q_t}{q_o}$$

These three sequential steps could be concluded from the Boyd's model like film diffusion process, particle diffusion and adsorption of the adsorbate. It show that adsorbate ions moves towards the surface of the adsorbent and travel within the pores of the adsorbent.

Adsorption Kinetics

The rate of adsorption process was determined by Lagergren's pseudo first order and Ho-McKay's pseudo-second order models. They are represented as:

$$ln(q_e - q_t) = lnq_e - k_1t$$

$$\frac{t}{q_t} = \frac{1}{k_2 q_e^2} + \frac{t}{q_e}$$

The representations of respective constants are described earlier. The values of rate constant and R^2 for the MGO sorption on Kaolin and Ag-KNC systems are represented in Fig. 10 and Table-2. The results show that the system follows the pseudo second order kinetics [47-53].
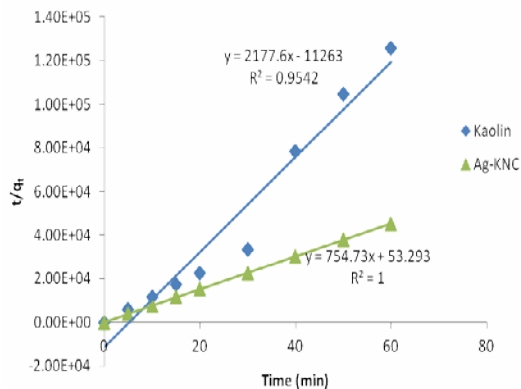
Fig. 10: Pseudo second order model of kinetics for kaolin and Ag-KNC -MGO System.

Table-2: Kinetic studies for the adsorption of MGO on Kaolin and Ag-KNC.

Adsorbents	Pseudo-second-order			Intra-particle-diffusion		q_e,Exp 10^{-4}(mg/g)
	k_2 10^2(g/mg.min)	q_e^2,theoretical 10^{-7}(g/mg)	R^2	$K_{i.d}$ (g/mg.min)	R^2	
Kaolin	4.30	2.151	0.953	8.542	0.704	2.79
Ag-KNC	74.8	17.60	0.996	9.274	0.620	13.3

Thermodynamic Parameters

The thermodynamic parameters: $\Delta G°$, $\Delta H°$ and $\Delta S°$ were calculated as:

$$lnK_D = \frac{\Delta S°}{R} - \frac{\Delta H°}{RT}$$

$$\Delta G° = \Delta H° - T\Delta S°$$

The values of $\Delta G°$ show spontaneous behavior of the system. The $\Delta H°$ values represent the exothermic behavior of the system. While the values of $\Delta S°$ were found to be positive[49]as shown in Table-3:

Photo Catalytic Effect for the Dye Removal

Mechanism of Photo Catalytic Degradation

The mechanism of photo catalytic degradation of MGO using Ag-KNC working as photo catalyst in the presence of UV irradiation is shown in Fig. 11.

It was observed that under UV illumination, Malachite green (MGO) dye absorbs radiations of desired wavelength and it was excited and giving its first excited singlet state. Beside this, the Ag-KNC also utilizes the evolved energy to excite its electron from valence band to the conduction band. The electron can be attracted from hydroxyl ion by (h^+) hole present in the valence band and generating • OH radical. This hydroxyl radicals will oxidize the MGO dye and its leuco form was observed by first doing ring aromatization which was followed by stabilization of the ion, which ultimately causes the degradation of the product [50, 51].

Optimum Parameters for the Removal of MGO by Photo catalytically

The optimum parameters for the removal of MGO dye was found to be 50 min and 1.20×10^{-5}M concentration as shown in Fig. 13.

Table-3: Thermodynamic Parameters for the adsorption of MGO on Kaolin and Ag-KNC at temperatures (298-313K)

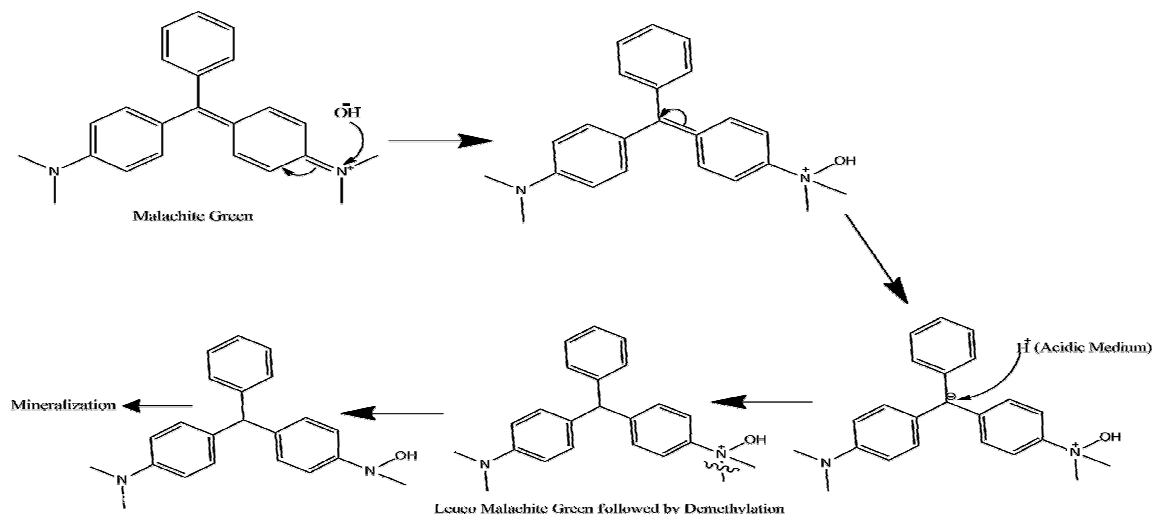| Adsorbents	Concentrations (mg L^{-1})	$\Delta H°$ (kJ.mol^{-1}.K^{-1})	$\Delta S°$ (J.mol^{-1}.K^{-1})	$\Delta G°$ (kJ.mol^{-1})			
				298K	303K	308K	313K
KAOLIN	50	-4.775	53.59	-3.724	-3.834	-3.896	-3.971
	100	-3.248	48.68	-3.740	-3.838	-3.904	-3.967
	150	-2.327	45.35	-3.715	-3.832	-3.885	-3.934
	200	-0.485	39.25	-3.717	-3.837	-3.872	-3.919
	300	-2.975	46.75	-3.637	-3.797	-3.884	-3.848
	500	-15.616	79.22	-2.871	-3.045	-3.217	-3.234
Ag-KNC	50	-4.031	24.32	-3.735	-3.818	-3.882	-3.871
	100	-0.188	37.49	-3.777	-3.825	-3.906	-3.959
	150	-0.841	35.34	-3.777	-3.831	-3.898	-3.956
	200	-1.162	34.10	-3.770	-3.815	-3.882	-3.944
	300	- 1.675	31.91	-3.734	-3.774	-3.877	-3.887
	500	-43.153	-111.45	-3.261	-3.496	-3.387	-2.747

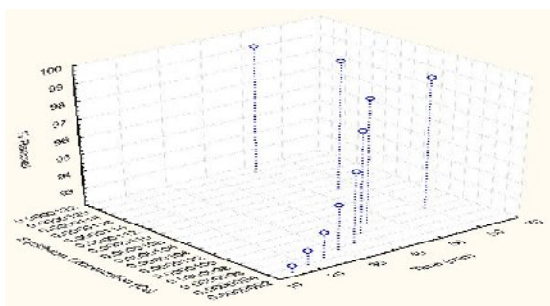Fig. 11: Mechanism of degradation of MGO Dye.

Fig. 12: 3D plot of % removal as a function of time and equilibrium concentration.

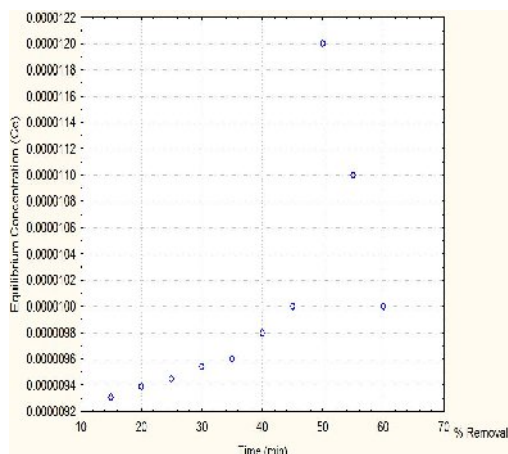The results are well agreed by contour plot to which is shown in Fig. 13.

Fig. 13: Contour plot of % removal as a function of time and equilibrium concentration.

The comparative removal efficiencies at variable temperatures are shown in Table-4. The result shows that at variable concentrations removal efficiencies was altered. At 100 mg/L and at 308K the maximum removal was observed to be 99.18 %. While at 500 mg/L removal was comparatively low, and system is more favorable at 100 mg/L concentration [52].

Table-4: Comparative Removal efficiency Of MGO-Ag-KNC System at Temperatures (298K-313K).

Concentration (mg L^{-1})	%Removal			
	298 K	303K	308K	313K
50	91.44	94.88	95.15	83.62
100	98.77	96.15	99.18	97.37
150	98.82	97.21	97.80	96.86
200	97.51	94.47	95.12	94.91
300	91.36	87.75	94.33	85.99
500	41.70	54.94	42.71	17.71

Conclusion

The present endeavor shows the synthesis of Kaolin assisted Ag nanocomposite. The SEM analysis represents that size of them within the range of 50 to 100nm. The EDS analysis represents the presence of respective metal. This study provides an efficient method for the treatment of textile waste water.

The adsorption and photo catalytic process were adopted for the removal of MGO dye. By the adsorption process about 95% removals was observed. While photo catalytic process shows 99% removal efficiencies.

The estimated data by adsorption process was incorporated to determine the rate constant by employing IPD and Ho-McKay's pseudo-second order models. The adsorption data represented that Freundlich isotherm was the best fitted model. The

thermodynamic parameters ΔG^o, ΔH^o and ΔS^o were evaluated, which represent the spontaneous and exothermic behavior of the system. The surface neutrality of the system at (pH_{pzc}) was also estimated. Effect of salt on the adsorption of dyes was estimated. The mechanism of the process was also elucidated.

In the light of current research work it can be concluded that, Keolin assisted Ag nanocomposite work as effective adsorbent and photo catalyst for the removal of dyes.

Conflict of interest

Author has no conflict of interest regarding the present studies.

References

1. X. Wang, J. Zhuang, Q. Peng, Y. Li, A general strategy for nanocrystal synthesis, *Nature*, **437**, 121 (2005).
2. S. Balci, A. M. Bittner, K. Hahn, C. Scheu, M. Knez, A. Kadri, C. Wege, H. Jeske, K. Kern, Copper nanowires within the central channel of tobacco mosaic virus particles, *Electrochim. acta*, **51**, 6251 (2006).
3. M. He, P. Huang, C. Zhang, F. Chen, C. Wang, J. Ma, R. He and D. Cui, A general strategy for the synthesis of upconversion rare earth fluoride nanocrystalsvia a novel OA/ionic liquid two-phase system, *Chem. Commun.*, **47**, 9510 (2011).
4. H. Tahir, U. Alam, Lignocellulosic: Non-Conventional Low Cost Biosorbent for the Elution of Coomassie Brilliant Blue (R-250), IJCR **6**, 56 (2014).
5. B. I. Nandapure, S. B. Kondawar, M. Y. Salunkhe, A I Nandapure, Magneticand Transport Properties of Conducting polyaniline/nickel Oxide Nanocomposites, *Adv.Mater.Lett.*,**4**, 134 (2013).
6. J. Yang, Carbon nanotubes reinforced composite for wind turbine blade. M. Sc Thesis, Case Western Reserve University, U.S., (2012).
7. G. V. Ramana, B. Padya, R. N. Kumar, K. V. P. Prabhakar, and. P. K. Jain, Mechanical properties of multi-walled carbon nanotubes reinforced polymer nanocomposites, IJEMS **17,** 331 (2010).
8. A. M. Marconnet, N. Yamamoto, M. A. Panzer, B. L. Wardle, K. E. Goodson, Thermal Conduction in Aligned Carbon Nanotube PolymerNanocomposites with High Packing Density*, ACS Nano*, **5**, 4818 (2011).
9. J. K. Mishra, Y. W. Chang, N. S. Choi, Preparation and characterization of rubber-toughened poly(trimethylene terephthalate)/organoclay nanocomposite, *Polym. Eng. Sci.*, **47**, 863 (2007).
10. S. Singh, K. C. Barick and D. Bahadur, Functional Oxide Nanomaterials and Nanocomposites for the Removal of Heavy Metals and Dyes, *Nanomater.Nanotechnol.*, **3**, 1 (2013).
11. K. Shameli, M. B. Ahmad, W. Z. W. Yunus., N. A. Ibrahim., M. Darroudi, Synthesis and characterization of Silver/Talc nanocomposites using the wet chemical reduction method, *Int. J. Nanomedicine*, **5**, 743 (2010).
12. S. Hashemian, M. R. Shahedi, Novel Ag/Kaolin Nanocomposite as Adsorbent for Removal of Acid Cyanine 5R from Aqueous Solution, *J. Chem.,* 1 (2013).
13. K. Shameli, M. B. Ahmad, M. Zargar, W. M. Z. W. Yunus, N. A. Ibrahim, P. Shabanzadeh, M. G. Moghaddam, Synthesis and characterization of silver /montmorillonite/chitosan bio nanocomposites by chemical reduction method and their antibacterial activity, *Int. J. Nanomedicine*, **6,** 271 (2011).
14. S. Meshrama, R. Limaye, S. Ghodke, S. Nigam, S. Sonawane and R. Chikate, Continuous flow photocatalytic reactor using ZnO–bentonite nanocomposite for degradation of phenol, *Chem. Eng. J.*, **172**, 1008 (2011).
15. Y. L. Liu, C. Y. Hsu, Y. H. Su and J. Y. Lai, Chitosan-silica complex membranes from sulfonic acid functionalized silica nanoparticles for pervaporation dehydration of ethanol-water solutions. *Biomacromolecules*. **6,** 368 (2005).
16. H. J. Zhai, D. W. Sun, H. S. Wang, Catalytic properties of Silica/Silver nanocomposites, *J. Nanosci. Nanotechnol.*, **6**, 1968 (2005).
17. A. Rapsomanikis, D. Papoulis, D. Panagiotaras, E. Kaplani, E. Stathatos, Nanocrystalline TiO_2 and halloysite clay mineral composite films prepared by sol-gel method: synergistic effect and the case of silver modification to the photocatalytic degradation of basic blue- 41 azo dye in water, *Glob. NES. J.*, **16**, 485 (2014).
18. V. K. Sharma, M. K. Siskova, and R. Zboril, Magnetic bimetallic Fe/Ag nanoparticles: Decontamination and antimicrobial agents." Interactions of nanomaterials with emerging environmental contaminants, Amer.

Chem. Soc. Symp. Ser., Publisher: Oxford University Press Volume **1150**, 193 (2013).

19. R. Rodiansono, T. Hara, S. Shimazu, Total hydrogenation of biomass-derived furfural over raney nickel-clay nanocomposite catalysts, *Indo. J. Chem*., **13**, 101 (2013).
20. A. M. Awwad, B. A. Albiss, N. M. Salem, Antibacterial activity of synthesized copper oxide nanoparticles using Malvasylvestris leaf extract, *SMU Med J*., **2**, 91 (2015).
21. S. Chatterjee, S. Chatterjee, B. P. Chatterjee, A. K. Guha, Adsorptive Removal of congo red, a carcinogenic textile dye by chitosan hydrobeads: Binding mechanism, equilibrium and kinetics, *Colloid surface A*, **299**, 146 (2007).
22. J. Singh, U. Sharma, S. Banerjee, Y. C. Sharma, A Very Fast Removal of Orange G from its Aqueous Solutions by Adsorption on Activated Saw Dust: Kinetic Modeling and Effect of Various Parameters *Int. rev. Chem. Eng*., **4**, 1 (2012).
23. A. B. Avagyan, Theory of Global Sustainable Development Based on Microalgae in Bio and Industrial Cycles, Management-Changing Decisions in Areas of Climate Change and Waste Management, JSBS, **3**, 287 (2013).
24. M. J. Iqbal, M. N. Ashiq, Adsorption of Dyes from Aqueous Solutions on Activated Charcoal, *J. Hazard. Mater*, **139**, 57 (2007).
25. G. L. Dotto, J. M. Moura, T. R. S. Cadaval, L. A. A. Pinto, Application of chitosan films for the removal of food dyes from aqueous solutions by adsorption, Chem. Eng. J., 214, 8 (2013).
26. D. Chatterjee, V. R. Patnam, A. Sikdar, S. K. Moulik, Removal of Some Common Textile Dyes from Aqueous Solution Using Fly Ash, *J. Chem. Eng. Data*, **55**, 5653 (2010).
27. R. B. Williams, and Environmental, U.S., Bentonite, kaolin and selected clay minerals. *Environm. Health Criteria*, **15,** 1 (2005).
28. H. Hassan, B. H. Hameed, Fenton-like Oxidation of Acid Red 1 Solutions Using Heterogeneous Catalyst Based on Ball Clay, *Int. J. Environ. Sci. Develop*., **2**, 218 (2011).
29. M. Saad, H. Tahir, F.Shaheen, Synthesis and characterization of SnO-CoOnanocomposits by bottom up approach and their efficacy for the treatment of dyes assisted simulated waste water, *Int. J. Curren. Res*., **7**, 23542 (2015).
30. G. A. Kraus, I. Jeon, M. Nilsen-Hamilton, A. M. Awad, J. Banerjee and B. Parvin, Fluorinated Analogs of Malachite Green*:* Synthesis and Toxicity*, Molecul., ***13(4)**, 986 (2008).

31. B. Sadeghi, S. Hashemian, Synthesis of Kaolin/Ag Nanocomposite as an Efficient and Versatile Reagent for the Synthesis of 1,8-Dioxo-Octahydroxanthene Derivatives, *Synth. React. Inorg. M*., **44**, 424 (2014).
32. G. Mustafa, H. Tahir, M. Sultan, N. Akhtar, Synthesis and characterization of cupric oxide (CuO) nanoparticles and their application for the removal of dyes, *Afr. J. Biotech*.,**12,** 6650 (2013).
33. K. S. Mantosh, B. Priya, D. J. Papita, Plant-mediated synthesis of silver-nanocomposite as novel effective azo dye adsorbent, *Appl. Nanosci.,* **5**, 1 (2013).
34. H. Tahir, M. Sultan and Z. Qadir, Physiochemical Modification and Characterization of Bentonite Clay and Its Application for the Removal of Reactive Dyes, *Int. J. Chem*., **5,** 19 (2013).
35. V. Vinayagam, P. Thangaraju, Equilibrium and Kinetics of Adsorption of Cationic Dyes by stishovite-Clay –TiO_2 Nanocomposite, *Int. J. Mod. Eng. Res*., **2**, 3989 (2012).
36. G. R. Mahdavinia and R. Zhalebaghy, Removal Kinetic of Cationic Dye Using Poly (Sodium Acrylate)-Carrageenan/Na-Montmorillonite Nanocomposite Superabsorbents, *Mater. Environ. Sci.,* **3,** 895 (2012).
37. F. C. Wu, R. L. Tseng and R. S. Juang, Initial behavior of intraparticle diffusion model used in the description of adsorption kinetics, *Chem. Eng. J*., **153,** 1 (2009).
38. M. H. Karaoğlu, M. Doğan and M. Alkan, Removal of cationic dyes by kaolinite, *Micropor. Mesopor. Mat*., **122,** 20 (2009).
39. T. Y. Jen, Y. C. Feng, C. J. C. Kuei, Kinetics and thermodynamics of adsorption for Cd on green manufactured nano-particles, *J. Hazard.Mater*.,**235,** 116 (2012).
40. J. S. Essomba, J. N. Nsami, P. D. B. Belibi, G. M. Tagne and J. K. Mbadcam, Adsorption of Cadmium(II) Ions from AqueousSolution onto Kaolinite and Metakaolinite, *Pure Appl. Chem. Sci*., **2**, 11 (2014).
41. G. Vijayakumar, R. Tamilarasan, M. Dharmendirakumar, Adsorption, Kinetic, Equilibrium and Thermodynamic studies on the removal of basic dye Rhodamine-B from aqueous solution by the use of natural adsorbent perlite, *J. Mater. Environ. Sci*., **3**, 157 (2012).
*42. H. Tahir, M. Sultan, Q. Jahanzeb, Remediation of azo dyes by using household used black tea as an adsorbent, *Afric. J. of Biotech., **8, **3584 (2009).*
43. A. O. Okewale, K. A. Babayemi and A. P. Olalekan, Adsorption Isotherms and Kinetics

Models of Starchy Adsorbents on Uptake of Water from Ethanol – Water Systems, *Int. J. Appl. Sci. Technol.*, **3**, 35 (2013).

44. W. H. Cheung, Y. S. Szeto, G. McKay, Intraparticle diffusion processes during acid dye adsorption onto chitosan*, Bioresource Technol.*, **98**, 2897 (2007).

45. B. H. Hameed, A. T. M. Din and A. L. Ahmad, Adsorption of methylene blue onto bamboo-based activated carbon: Kinetics and equilibrium studies, *J. hazard. Mater.*, **141**, 819 (2007).

46. I. Tsibranska and E. Hristova, Comparison of different kinetic models for adsorption of heavy metals onto activated carbon from apricot stones, *Bulgarian Chem. Comm.*, **43,** 370 (2011).

47. O. Okewale, K. A. Babayemi, A. P. O. lalekan,, Adsorption Isotherms and Kinetics Models of Starchy Adsorbents on Uptake of Water from Ethanol – Water Systems *Intern. Journ. Appl. Scien. Technology*, **3**, 9 (2013*).*

48. W. H. Cheung, Y. S. Szeto, G. McKay, Intraparticle diffusion processes during acid dye

adsorption onto chitosan, *Biores. Techn.*, **98**, 2897 (2007).

49. M. Anbia, and M. Haqshenas, Adsorption studies of Pb(II) and Cu(II) ions on mesoporous carbon nitride functionalized with melamine-based dendrimer amine. *Intern. Journ. of Environmen. Scien. and Techn.*, **12**, 2649 (2015).

50. S. Pal, A. M. Laera, A Licciulli, M. Catalano, and A. Taurino, Biphase TiO_2 microspheres with enhanced photocatalytic activity. *Industrial & Engineering Chemistry Research*, **53**, 7931 (2014).

51. H. Tahir, M. Sultan, N. Akhtar, U. Hameed and T. Abid, Application of natural and modified sugar cane bagasse for the removal of dye from aqueous solution, *J. of Saud. Chemic. Soc.*,, **20**, S115 (2016).

52. A .Gautam, A. K. shirsagar, R.Biswas, S. Banerjee, PK. Khanna, Photodegradation of organic dyes based on anatase and rutile TiO_2 nanoparticles. *RSC Advances,.***6**, 2746 (2016).